

A Galaxy-Weighted Measure of the Relative Peculiar Velocity Dispersion

Marc Davis

Depts. of Astronomy and Physics, Univ. of California, Berkeley
marc@coma.berkeley.edu

Amber Miller

Dept. of Physics, Princeton University
amber@pupgg.princeton.edu

and

Simon D.M. White

MPI fuer Astrophysik, Garching
swhite@mpa-garching.mpg.de

Abstract

The relative pair dispersion of galaxies has for the past decade been the standard measure of the thermal energy of fluctuations in the observed galaxy distribution. This statistic is known to be unstable, since it is a pair-weighted measure that is very sensitive to rare, rich clusters of galaxies. As a more stable alternative, we here present a single-particle-weighted statistic σ_1 , which can be considered as an estimate of the one-dimensional rms peculiar velocity dispersion of galaxies relative to their neighbors, and which can be interpreted by means of a filtered version of the Cosmic-Energy equation. We calculate this statistic for the all-sky survey of IRAS galaxies, finding $\sigma_1 = 95 \pm 16$ km/sec. The UGC catalog yields a higher value, $\sigma_1 = 130 \pm 15$ km/s. We calibrate our procedure by means of mock catalogs constructed from N-body simulations and find that our method is stable and has modest biases which can easily be corrected. We use the measured values of σ_1 in a filtered Layzer-Irvine equation to obtain an estimate of $\tilde{\Omega} \equiv \Omega/b^2$. We find that $\tilde{\Omega} \approx 0.14 \pm 0.05$ for both the IRAS and UGC catalogs, which is slightly lower than other recent determinations, but is consistent with a trend of an effective Ω that increases gradually with scale.

1. Introduction

Considerable effort has been devoted in the past decade to the measurement of the quantity $\sigma_{12}(r)$, the relative peculiar velocity dispersion of pairs of galaxies as a function of their separation (Davis et al 1978; Peebles 1979, 1981; Davis and Peebles 1983, hereafter DP83; Bean et al 1983; de Lapparent et al 1988; Hale-Sutton et al 1989; Mo et al 1993; Zurek et al 1994; Fisher et al 1994a; Marzke et al 1995; Brainerd et al 1996, Somerville *et al.* 1996). The relative pair velocity dispersion is most easily extracted from the two-point correlation function in redshift space, $\xi(r_p, \pi)$. Since this correlation is a pair-weighted quantity, so is the rms peculiar velocity dispersion. Dense clusters of galaxies contain many pairs and have high internal velocity dispersion. Consequently they can dominate the measured dispersion, as shown by Mo et al. (1993), Zurek et al. (1994), and Somerville *et al.* (1996), who found that the elimination of the cores of dense clusters leads to a significant reduction in the measured σ_{12} and argued that the “true” value might be substantially larger than earlier estimates. For these reasons, many authors (Hale-Sutton et al 1989; Mo et al. 1993; Zurek et al. 1994; Guzzo et al. 1996) have concluded that this statistic is unreliable. It is possible that a reliable estimate has finally been achieved with the nearly complete CfA2 survey (Marzke et al 1995), but until these results are confirmed by even larger surveys, a cloud of uncertainty will remain.

The relative pair dispersion $\sigma_{12}(r)$ is well defined from the point of view of kinetic theory (Davis and Peebles 1977, Peebles 1980) and is an essential ingredient in the cosmic virial theorem (CVT), which is itself a statement of equilibrium between kinetic pressure and gravitational acceleration averaged across all virialized systems. The proper evaluation of the cosmic virial theorem includes a nearly divergent integral over the poorly constrained 3-point correlation function of galaxies ζ (see Peebles 1980, eq. 75.10). Comparison of σ_{12} to this integral yields a measure of the cosmic density parameter Ω , subject to all the usual arguments about bias in the galaxy distribution. The sensitivity of σ_{12} to the treatment of the rare dense clusters is very likely matched by similar sensitivity in the integral over ζ , but this has never been checked directly. Juszkiewicz and Yahil (1989) have shown how the standard CVT, which applies to nonlinear clustering on small scales, can be readily extended to the linear regime valid on large scales. Mo *et al.* (1996) have shown how analytical approximations to σ_{12} and to other low order statistics can be derived from the initial linear power spectrum $P(k)$. Bartlett and Blanchard (1993, 1996) have pointed out that the integral of the three-point function ζ should be taken over the *galaxy-galaxy-mass* correlations, and that the usual estimate of ζ based on *galaxy-galaxy-galaxy* correlations can seriously underestimate the inferred Ω , if galaxies have extended massive halos. Kepner *et al.* (1996) have suggested that much of sampling variance of σ_{12} is likely to be reduced if it is tabulated as a function of the galaxy density surrounding each pair.

Although the CVT test for Ω is rarely performed with any rigor, $\sigma_{12}(r)$ for the mass distribution is easily measured in high resolution N-body simulations, and is often used to compare them with observation (e.g. Davis et al 1985). The fact that the observed pair dispersion in the galaxy distribution is well below that expected for the mass distribution in an $\Omega = 1$ cosmology was the major factor motivating the concept of bias in the galaxy distribution. Considerable attention has been given to the distinction between $\sigma_{12}(r)$ measured for galaxies and the same quantity measured for the mass in simulations (e.g. Davis et al 1985; Couchman et al 1990; Gelb and Bertschinger 1994; Zurek et al 1994). The results are, not surprisingly, very sensitive to the spatial resolution of the simulation and to the degree to which clumps of dark matter in the simulations are separated into distinct “galaxies”.

There is clearly a need for a simple statistic to evaluate the kinetic energy of the galaxy distribution, preferably one that is both easily evaluated and stable. In this paper, we develop a statistic which contains much of the same information as σ_{12} but is galaxy-weighted rather than a pair-weighted. We describe the statistic and its theoretical underpinning in Section 2, and apply it to several redshift survey catalogs in Section 3. We demonstrate the robustness of our statistic by applying it to a series of mock catalogs extracted from a high resolution N-body simulation. We believe that it will prove both robust and useful in diagnosing the thermal state of the galaxy distribution.

2. Cosmic Energy

2.1. The Standard Layzer-Irvine Equation

Consider the cosmic energy equation, also known as the Layzer-Irvine equation, which describes the relationship between the kinetic and potential energies of the fully-nonlinear fluctuation field. Consider a sample with mass $M = \sum m_i = \rho_b V$ where $\rho_b = 3\Omega H_0^2/8\pi G$ is the mean matter density. The specific kinetic K energy in fluctuations can be written as a sum over the particles

$$K = \frac{\rho_b}{2M} \int d^3x (1 + \delta(\mathbf{x})) (\bar{\mathbf{v}}^2(\mathbf{x}) + \sigma^2(\mathbf{x})) = \frac{3}{2} \langle v_p^2 \rangle \quad (1)$$

where $\delta(\mathbf{x})$, $\bar{\mathbf{v}}(\mathbf{x})$ and $\sigma(\mathbf{x})$ are the overdensity and the mean and dispersion in peculiar velocity of the particles at position \mathbf{x} , and $\langle v_p^2 \rangle^{1/2}$ is the one-dimensional peculiar velocity dispersion averaged over all particles. The specific potential energy W is given by

$$W = -\frac{Ga^2\rho_b^2}{2M} \int d^3x_1 d^3x_2 \delta(\mathbf{x}_1)\delta(\mathbf{x}_2)/x_{12} = -2\pi G\rho_b J_2 \quad (2)$$

where $x_{12} = |\mathbf{x}_1 - \mathbf{x}_2|$ and J_2 is given by the usual expression, $J_2 = \int \xi(r)rdr$ with $\xi(r)$ the two-point correlation function of the mass distribution. Thus

$$W = -\frac{3}{4}\Omega H_0^2 J_2. \quad (3)$$

The Layzer-Irvine equation is an exact result relating the time evolution of K and W ,

$$\frac{dK}{dt} + \frac{dW}{dt} + \frac{\dot{a}}{a}(2K + W) = 0 \quad (4)$$

(Peebles 1980 eq. [24.7]), where a is the expansion parameter.

In the limit of self-similar clustering, equation (4) reduces to an algebraic expression (Peebles 1980 eq. [74.6], DP83 eq. [33]),

$$K = \frac{4}{7+n}|W| \quad (5)$$

where n is the index of the linear power spectrum, $P(k) \propto k^n$. In applications to real data one might take $n \approx -1$, the effective slope of the power spectrum on the scale of nonlinear clustering, i.e. near $8 \text{ h}^{-1} \text{ Mpc}$. Note that for $n = -1$ equation (5) gives $K/|W| = 2/3$, which, as we show below, is the value expected for linear clustering in an Einstein-de Sitter universe with any power spectrum. In an open universe with no growing modes and only stable virialized

clusters, the Layzer-Irvine equation becomes $K/|W| \approx 1/2$. Thus we can encompass the likely range of possibilities for our Universe by writing Eq (5) as

$$\langle v_p^2 \rangle \approx g\Omega H_0^2 J_2 \quad (6)$$

where g is in the restricted range $1/4 < g < 1/3$.

This form of the Layzer-Irvine equation was first used by Fall (1976) to set constraints on Ω based on the Shapley-Ames redshift catalog. If we approximate $\xi(r)$ by a power law, $\xi(r) = (\frac{r}{r_0})^{-\gamma}$ with a cutoff at $r > xr_0$, then we expect a one-dimensional rms peculiar velocity

$$\langle v_p^2 \rangle^{1/2} = \Omega^{1/2} \left(\frac{gx^{2-\gamma}}{(2-\gamma)} \right)^{1/2} H_0 r_0 \approx 1.4\Omega^{1/2} H_0 r_0 \quad (7)$$

where the last equality results from $\gamma = 1.8$, $x = 4$, and $g = 1/3$. Thus in an $\Omega = 1$ Universe in which galaxies trace the mass with $H_0 r_0 = 500$ km/s, the 1-d rms velocity of particles relative to the comoving frame is expected to be quite large, 700 km/s, corresponding to an *rms* three-dimensional velocity of 1200 km/s. This can be compared with the peculiar velocity of our own galaxy, 620 km/s.

There are several well known problems with equation (7) that have prevented its widespread application in cosmology. First note that the integrand of J_2 is divergent at large scale for a power law correlation function; the convergence of the integral is dependent on the uncertain turnover scale from pure power law behavior, which is only weakly constrained, and therefore J_2 is poorly determined. Furthermore, $\langle v_p^2 \rangle^{1/2}$ is the rms velocity of matter relative to the comoving frame, but this quantity can be reliably measured only for the Milky Way. The Layzer-Irvine equation is a very simple statistic that applies on a global scale; it is an average of the energy balance across all scales. The kinetic energy term includes nonlinear motion within groups as well as large scale, coherent flows. Similarly, the potential term is an integral of the fluctuations on all scales both large and small. The problem in the application of the cosmic energy equation is that reliable measurements of the largest scale contributions are not available for either the kinetic or potential energy terms.

2.2. A Filtered Version of the Cosmic Energy Equation

The problems with the cosmic energy equation can be overcome if we consider a filtered version of both K and W . The Fourier decompositions of the density contrast and the mean peculiar velocity are

$$\begin{aligned} \delta(\mathbf{x}) &= \frac{1}{(2\pi)^3} \int d^3k \delta_{\mathbf{k}} e^{i\mathbf{k}\cdot\mathbf{x}} \quad , \\ \bar{\mathbf{v}}(\mathbf{x}) &= \frac{1}{(2\pi)^3} \int d^3k \bar{\mathbf{v}}_{\mathbf{k}} e^{i\mathbf{k}\cdot\mathbf{x}} \quad . \end{aligned} \quad (8)$$

The large-scale but small amplitude fluctuations in density which make it difficult to evaluate J_2 are represented by the small k Fourier components $\delta_{\mathbf{k}}$ and the large-scale streaming motions to which they give rise are represented by the small k components $\bar{\mathbf{v}}_{\mathbf{k}}$. According to late-time linear theory (Peebles 1980) these two quantities are related by

$$\bar{\mathbf{v}}_{\mathbf{k}} = H_0 f(\Omega) \frac{\delta_{\mathbf{k}}}{i\mathbf{k}} \quad , \quad (9)$$

where to a good approximation $f(\Omega) = \Omega^{0.6}$. The corresponding contributions to W and K can be written as

$$W_k = \frac{Ga^2 \rho_b}{(2\pi)^2 V} \frac{|\delta_k^2|}{k^2} \quad (10)$$

and

$$K_k = \frac{1}{2V(2\pi)^3} |\mathbf{v}_k|^2, \quad (11)$$

so that in linear theory K_k and W_k are related by

$$K_k = \frac{2f^2(\Omega)}{3\Omega} |W_k|. \quad (12)$$

Since this is true for each linear mode, we see that

$$K/|W| \approx 0.667\Omega^{0.2} \quad (13)$$

holds for the entire large-scale linear contribution to the Layzer-Irvine equation.

This suggests that we consider a filtered version of equation (6) with these uncertain large-scale contributions removed:

$$\tilde{v}_p^2 \approx \tilde{g}\Omega H_0^2 \tilde{J}_2 \quad (14)$$

where \tilde{v}_p^2 and \tilde{J}_2 are high spatial frequency versions of the rms peculiar velocity and potential energy and \tilde{g} is a modified scaling constant that could be somewhat scale-dependent.

To be safe we would like to remove large-scale contributions only on scales where we are sure the distribution is linear. However, with available data sets, it is necessary to filter on relatively small scales to have acceptable signal to noise in the resulting statistics. To test how well equation (14) works as a function of filtering scale, we examined the output from several high resolution PPPM N-body simulations. We have studied one simulation with $n = -1$ power law initial fluctuations and $\Omega = 1$, and another with $n = -1$ and $\Omega = 0.1$, both with 10^6 particles and with size of $\approx 200h^{-1}$ Mpc. We have also examined a simulation of 2×10^6 particles with CDM initial conditions and $\Omega = 1$. Table 1 gives values $K/|W|$ as a function of filtering scale for these simulations. We use a gaussian filter to smooth the potential energy in Fourier space and the velocities in real space. We give the scale of the gaussian filter, σ_s , in units of the matter correlation length, r_0 , and we list the kinetic energy density in small scale motions for the $\Omega = 1$, $n = -1$ model (in arbitrary units). Finally for each model we give the ratio $K/|W|$ both for the high frequency structure retained in equation (14) and for the large-scale contributions which have been removed. Notice that for both $n = -1$ models the large-scale ratio approaches the value expected from equation (13) as the smoothing is increased, but that the CDM model is still far from the linear prediction on the largest scale considered.

One expects \tilde{g} to be scale-dependent because on sufficiently small scale the filtered kinetic energy will be larger than the filtered potential energy, implying merely that the systems are not bound on that scale. This is equivalent to the situation within galaxies: stars orbiting within a 10 kpc elliptical galaxy are not bound by the mass distribution on a 1 kpc scale. On the other hand, $\tilde{g} \approx 1/4$ is a likely lower bound consistent with virial equilibrium on small scales, and thus can provide an upper limit to the derived density Ω . The physical interpretation of the filtered cosmic energy equation is simply that there is a balance between potential and kinetic energy provided all scales are included up to those of the largest virialized systems. The great advantage of the filtering is that, by deleting the long wavelength modes, the kinetic energy

term can be measured by the motion of galaxies relative to their neighbors; common large-scale motions need not be considered. The filtered value of W is easily calculated as a suitably filtered version of the correlation function integral J_2 . The small-scale values of $K/|W|$ in Table 1 are only slightly model-dependent, so there is little ambiguity in applying equation (14).

In the next section, we show how to construct a suitably filtered velocity dispersion. We proceed by constructing the relative distribution of pairs because this can be done using redshift information alone and automatically filters out common motions. To prevent this statistic from being pair weighted as in the σ_{12} analysis, we shall construct a mean distribution function of relative velocities in which each galaxy is given equal weight.

3. A Galaxy Weighted Velocity Statistic

3.1 The Samples

The primary data we shall use comes from an all sky redshift survey of galaxies from the Infrared Astronomical Satellite (IRAS) data base, flux limited to 1.2 Jy at 60μ (Fisher et al 1995). We semi-volume limit the sample by deleting galaxies with 60μ flux too low for them to be included in the sample if they are placed at a redshift of 4000 km/sec, and we truncate the sample at redshift 8000 km/s. The IRAS sample thus selected contains 2374 galaxies. We do not consider cosmic flow fields in constructing this subsample, presuming redshifts in the LG frame to be equivalent to distances. We also examine a sample of 1959 optical galaxies taken from the Uppsala General Catalog (UGC) with $m < 14.5$ and $b > 30^\circ$, using the same volume limit and redshift limit as for the IRAS catalog. This UGC catalog is a subsample of the recently completed ORS redshift survey (Santiago et al 1995, 1996).

3.2 Building the distribution of relative velocities

Consider a galaxy in the catalog. We consider any other galaxy with projected separation less than a limiting value r_p and with a redshift separation of less than 1200 km/s to be a neighbor of the original galaxy. The distribution P of observed δz as a function of pair separation is constructed for each galaxy individually along with the smoothed expected background distribution based on the selection function and density for each sample. Thus if the catalog's selection function is $\phi(v)$ and the mean density is \bar{n} , then the expected smooth background at redshift separation $\pm\Delta v$ from a galaxy at measured redshift v is simply

$$B(\Delta v) = f_B \pi r_p^2 \delta v \bar{n} \phi(v \pm \Delta v) \quad (15)$$

where f_B is a fraction of the area of the projected circle that falls within the catalog boundaries, and $\delta v = 50$ km/s is the width of the binning in redshift space. This background distribution B is then subtracted from the pair distribution P and the resultant distribution is normalized by the difference between the total number of real pairs and the total number of pairs expected from a the background distribution. That is, for each galaxy we construct a statistic G given by

$$G(\Delta v) = \frac{P(\Delta v) - B(\Delta v)}{\sum_{\Delta v} (P(\Delta v) - B(\Delta v))} \quad (16)$$

where the summation is taken over the bins of redshift separation.

The total distribution, $D(\Delta v)$, is built by adding together the individual galaxy distributions, $D(\Delta v) = \sum_n G_n(\Delta v)$. This procedure normalizes the distribution of pairs around each galaxy by the total number of excess pairs for that galaxy, rather than equally weighting all galaxy pairs. Only galaxies for which the total number of pairs exceeds the total background by at least one are included in the summation defining D . By deleting the galaxies with fewer pairs than expected at random, we bias the distribution toward the denser regions, but this bias can be readily corrected. An alternative might be to accumulate the normalized $P(\Delta v)$ statistic, with no individual background subtraction, but then the background subtraction from $D(\Delta v)$ would be problematic since the expected background is not the same for each galaxy in the catalog.

The resulting distributions for the IRAS, UGC, and (uncooled) N-body data sets are plotted in Figure 1. These curves simply represent the probability that a random galaxy has excess neighbors with a given projected separation and redshift separation (velocity difference) Δv . Since we know that galaxies are correlated in real space, we would expect this distribution function to have a non-zero width even in the absence of redshift space distortions. Interpretation of this distribution function in terms of random peculiar motions is described below.

3.3 Mock Catalog Samples

In order to gain a better understanding of what is being measured in this procedure, we make extensive use of an N-body mock catalog generated from a high resolution N-body simulation of 10^6 particles with $\Omega = 1$ and with power law spectral index $n = -1$. The method by which the mock catalogs are generated is discussed in Fisher et al (1994b) and Davis, Nusser, Willick (1996). This sample, which is unbiased relative to the mass, is similarly flux limited and contains 4092 “galaxies”. We have chosen a scaling of the simulation such that the correlation length r_0 closely matches that of the IRAS catalog, $r_0 \approx 3.6h^{-1}$ Mpc.

We shall find that the measured value of the dispersion obtained for the N-body catalog differs significantly from that obtained for the IRAS and UGC catalogs. This is not unexpected because it is known that the N-body simulations produce small-scale velocity fields much hotter than those observed. In order to produce models that mimic the observations, the velocity fields in these simulations are often smoothed using a Gaussian window function (Fisher et al 1994b). In the present case, however, it is important not to alter the distribution function of peculiar velocities on small scales. Instead of smoothing the velocity field, we transform the N-body galaxies to real space using the known individual peculiar velocities, and then divide those peculiar velocities in half before transforming back into redshift space. This procedure has the advantage that it reduces the velocity dispersion without changing the shape of small-scale distribution. Thus we have both a hot and a cooled version of the same mock catalog which we shall use in the analysis below. Although this is admittedly not a self-consistent procedure for constructing the Universe, it does provide a fair test of our ability to recover the amplitude of the small-scale velocity field in the presence of strong clustering.

We also examined a series of mock catalogs which were cooled in the fashion described by Davis, Nusser, and Willick (1996), in which a smoothed version of the velocity field is averaged with the original velocity field. This has the effect of preserving the original amplitude of the large scale flows and of diminishing the small scale velocities by a factor of two. We find that this more sophisticated cooling yields very similar results to the simpler cooling procedure.

The N-body models can also be used to demonstrate the separation of large and small-scale peculiar motions. Our velocity statistic is sensitive to the small-scale peculiar motions, the motion of neighboring galaxies relative to each other. But a substantial fraction of the peculiar motion of galaxies is coherent on small scales and is a common-mode, bulk flow motion that is filtered out by our procedure.

To study this separation, we make use of the true peculiar velocity information provided by the mock IRAS, N-body catalogs to transform the mock samples from redshift space to real space. Consider the set of “galaxies” that have excess neighbors within a sphere in real space of radius $r_s = 2h^{-1}$ Mpc. The solid curve of Figure 2 shows the peculiar velocity distribution of these points, relative to the comoving frame of the simulation. Note that the distribution is asymmetric, with long tails. The asymmetry is a consequence of the anisotropic distribution of the galaxies in the mock catalog, which has been carefully designed to mimic the actual IRAS survey with its large-scale flows and large motion (600 km/s) of the central observer. The dashed curve in Figure 2 shows the peculiar velocity distribution of these same points relative to the mean peculiar velocity of their neighbors within the same sphere. The common-mode, bulk flow motion has been removed, and the distribution is now symmetric about zero, with a much narrower width and modest tails.

For a larger neighbor window, we might expect the internal velocity dispersion to increase, while the rms of the external (or bulk flow) peculiar velocity dispersion should decrease. We examine “galaxies” with neighbors within real space spheres of radius ranging from $1h^{-1}$ Mpc to $5h^{-1}$ Mpc with results for the internal and bulk flow dispersion given in Table 2. These dispersions do NOT behave in the naively expected manner; we find that the rms of the external (bulk flow) peculiar velocity dispersion does decrease with increasing scale but so does the internal velocity dispersion, in contrast to the behavior of the simulation as a whole, as given in Table 1.

The fourth column in Table 2 is the true rms value of the peculiar velocity (relative to the comoving frame) for all the points having neighbors within the selection radius. This column provides an explanation of the behavior of the dispersions measured as a function of scale. We see that the galaxies entering into our analysis are not a fair sample of the total population as measured by the rms dispersion. The galaxies with pairs on increasingly small scales represent a more and more biased subsample of all the points; the selected ‘galaxies’ with pairs are preferentially found in the denser regions, which have higher peculiar velocities. This effect can also be seen by making maps of the galaxies on “redshift shells”, maps of the galaxies on the sky which have redshifts between two limiting values. Galaxies with peculiar velocities larger than 1000 km/sec tend to be located within the denser regions of the maps. Because we are working with flux limited catalogs, galaxies at higher redshifts having pairs are even more biased than galaxies at lower redshift.

The bias so induced can be estimated from the fifth and sixth columns of Table 2. Here we list the fraction of mock points having real space neighbors within a given scale, along with the ratio of the rms peculiar velocity of these points relative to all the points in the mock catalog. Note that less than half of the “galaxies” have neighbors within $2h^{-1}$ Mpc and that these points have slightly higher than average velocity dispersion.

Since the true peculiar velocities are not known for the IRAS or UGC galaxies, these catalogs cannot be converted to real space. Therefore for direct comparison with the IRAS or UGC distributions, it is essential to go back to redshift space. In redshift space, galaxies having fewer neighbors than expected from a random background are excluded from analysis

as described above. Table 3 shows the fraction of galaxies included in the analysis for each catalog. The Table also shows the ratio of the rms dispersion of galaxies in the analysis to the rms dispersion of all the galaxies in the catalog. This latter quantity can be directly measured only for the mock catalog.

Fortunately a nearly identical fraction of galaxies within the IRAS, UGC, and the N-body samples have neighbors in excess of the random background, and we shall therefore assume that the ratio of the dispersions behave similarly. We thus shall decrease the measured value of the IRAS and UGC dispersions by a factor of 1.19, the value obtained for the mock catalog in Table 3.

3.4 Measurement of the intrinsic dispersion, σ_I

For the analysis in redshift space, we have chosen pairs to be galaxies separated by up to $2 \text{ h}^{-1} \text{ Mpc}$ projected separation and 1000 km/sec along the line of sight. The distribution $D(\Delta v)$ describes the distribution function the radial velocity of neighbors in excess of random, summed over all galaxies in the sample. Because galaxies are clustered the second moment of the distribution of D would be nonzero even in the absence of peculiar velocities. The density of neighboring galaxies expected in excess of a randomly chosen galaxy is simply proportional to the two point correlation function $\xi(r)$. In order to interpret the measured $D(\Delta v)$, we note that the observed redshift space correlation function is a convolution of the true spatial correlation function $\xi(r)$ with a velocity distribution function, which we can write as

$$\xi(r_p, \pi) = C \int \frac{dy}{\sigma_I(r)} \xi(r) \exp\left(-\eta \left|\frac{\pi - y}{\sigma_I(r)}\right|^\nu\right) \quad (18)$$

where $r = \sqrt{r_p^2 + y^2}$ (Fisher *et al.* II eq. [12]). Fisher *et al.* note that both the pair weighted velocity distribution functions for the IRAS data and the N-body models are adequately fit by an exponential model ($\eta = \sqrt{2}$, $C = 1/\sqrt{2}$, and $\nu = 1$). There is no guarantee, however, that an exponential model will yield the best fit to the new particle weighted distribution function, and we have tested gaussian models ($C = 1/\sqrt{2\pi}$, $\eta = 1/2$, and $\nu = 2$) as well. With these choices of η , σ_I is the rms dispersion of galaxies relative to their neighbors in both the exponential and gaussian models. We define $\sigma_I(r)$ to be the intrinsic dispersion, and set it to be constant in r . We furthermore ignore streaming effects of the sort discussed by DP83 and Fisher *et al.* II, since we are interested in the mean velocity dispersion around individual galaxies, not the mean streaming and velocity dispersion of pairs of galaxies. Thus we construct a model velocity distribution function $M(\pi)$ as

$$M(\pi) = \frac{2\pi C_1}{\sigma_I} \int_0^{2h^{-1}} dr_p r_p \int_{-\infty}^{\infty} dy \xi(r) \exp\left(-\frac{\eta}{\sigma_I} |\pi - y|^\nu\right). \quad (19)$$

The normalizing constant C_1 depends on the selection function and redshift distribution of the galaxies with neighbors in the sample but it will scale out of the analysis. Thus only the shape, and not the amplitude, of two point correlation function is required for the modeling of $D(\Delta v)$. For the IRAS and UGC data, the function, $\xi(r)$ is well defined by a power law,

$$\xi(r) = \left(\frac{r_o}{r}\right)^\gamma, \quad (20)$$

where $r_o = 3.76 \text{ h}^{-1} \text{ Mpc}$ and $\gamma = 1.66$ for IRAS (Fisher et. al I), while $r_o = 5.4 \text{ h}^{-1} \text{ Mpc}$ and $\gamma = 1.8$ for the UGC (DP83). The integral is easily evaluated numerically. The N-body case is more complicated because the correlation function is poorly fit by a power law and has to be treated with more care. The correlation function $\xi(r)$ for the full N-body simulation was measured and used in the evaluating the integral Eq (19) numerically.

Before estimating the intrinsic dispersion σ_I , we found it necessary to first subtract the average of the measured $D(\Delta v)$ for the range $1000 < \Delta v < 1200 \text{ km/s}$ from the full distribution $D(\Delta v)$. This correction removes small biases that affect the measured $G(\Delta v)$ for each galaxy (Eq. 16) by our requirement that each galaxy have neighbors in excess of random; fluctuations of randomly distributed background galaxies can, on occasion, populate a long tail in the $G(\Delta v)$ distribution and would bias the inferred dispersion. For a given σ_I , we can construct model distribution function $M(\Delta v)$, again with $\bar{M}(1000 < \Delta v < 1200)$ subtracted from the distribution. We shall denote subscript c for background subtracted distributions. We furthermore adjust the model normalization C_1 such that

$$\int_0^{1000} D_c(\Delta v) d\Delta v = \int_0^{1000} M_c(\Delta v) d\Delta v \quad . \quad (21)$$

To determine a best fitting model from these corrected distributions, we simply evaluate the sum of the squared deviation,

$$\chi^2 = \sum_i \left(\frac{D_c(\Delta v_i) - M_c(\Delta v_i)}{N_i} \right)^2 \quad , \quad (22)$$

where N_i is the uncertainty of point i . We have chosen N_i constant but find little change in the best σ_I for different weightings.

The measured velocity distribution is plotted in Figure 3 for each catalog, along with the best fitting exponential and gaussian models; also shown are fits with $\sigma_I = 0$. The solid curve in each case is the same as in Figure 1, apart from the adjustment of the zero point. The effects of the velocity broadening are clearly observable. Results for the inferred value of σ_I are listed in Table 4 for gaussian and exponential models, with the model leading to the best χ^2 given in boldface. The UGC catalog is best fit with an exponential model (i.e. the best χ^2 is substantially lower), while the IRAS and N-body catalogs have lower χ^2 when using the gaussian velocity distribution. It is not too surprising that the real catalogs would behave this way, since the IRAS catalog undersamples the richer regions of the UGC survey, and thus would be expected to have less of a tail in the distribution. It is unclear why the N-body catalogs, sampling a similar volume to the IRAS survey, do not similarly favor the exponential models.

Note that the inferred σ_I does indeed drop by a factor of ≈ 2 between the cooled and uncooled simulation, as expected. This is a demonstration that our statistical procedure is sensible, and the test is not trivial since the selection of neighbors is performed in *redshift space*. The uncooled N-body model is so hot, however, that our estimate of σ_I is compromised by the relatively small window in velocity space from which we draw the neighbor pairs. The derived σ_1 for the cooled N-body model, 192 km/s , can be compared to the internal dispersion of the N-body models listed in Table 2, $\approx 450 \text{ km/s}$ for pairs within $2h^{-1} \text{ Mpc}$. Dividing this value by the same factors for the artificial cooling and bias ($2*1.19$) leads to an expected $\sigma_1 = 189 \text{ km/s}$, exactly as measured in redshift space.

The statistical errors given in Table 4 are the one sigma error contours derived from the χ^2 procedure. Assuming the best fit to be acceptable over the twenty bins of data with two degrees of freedom (σ_I and the overall normalization), we list the change in σ_I that increments χ^2 by 1/18 of its minimum value.

An independent estimate of the errors can be derived by a Monte Carlo experiment. We have constructed five independent mock IRAS catalogs from the same large N-body simulation and have cooled their velocity fields by the method described by Davis *et al.* 1996. Each of these simulations have similar size and sampling density to the IRAS catalog. Comparison of the individual estimates of σ_I for these mock catalogs simulates all the statistical effects of our procedure, including sampling variance. The dispersion of the best σ_I measured from the five mock catalogs is only 30 km/s, or 9%, which is consistent with the errors listed in Table 4.

In Table 4, we also list σ_1 , the final value of the single particle one dimensional dispersion, which is simply σ_I corrected for the selection bias factor of 1.19 discussed above and by a factor of $\sqrt{2}$ to change from the rms of the difference between two galaxies to the motion of a single galaxy. Each σ_1 listed is based on the better of the gaussian/exponential fits. The numbers in boldface highlight the preferred models, either exponential or gaussian, that has the smaller χ^2 . The lower dispersion for the IRAS galaxies is hardly a surprise, given that this catalog, relative to optically selected samples such as the UGC, undercounts elliptical and lenticular galaxies that are most abundant in the dense, hot cluster regions. But note that even the UGC catalog leads to a dispersion considerably less than that obtained from the *artificially cooled* N-body models.

Our object weighted velocity dispersion is similar to that defined by Rivolo and Yahil (1981). The final quantity, σ_1 , is itself very similar to the mean velocity dispersion within groups of galaxies (e.g. Nolthenius and White 1987; Ramella, Geller, and Huchra 1989; Nolthenius, Klypin, and Primack 1994). In fact, the method should yield virtually the same result because only galaxies in groups have neighbors above the background level. Our analysis is distinct from those recent analyses that focus on the kinematics of dwarfs around isolated large galaxies (e.g. Zaritsky and White 1994, Zaritsky *et al.* 1996). The information we have obtained tells us nothing about the dispersion versus environment, as measured by e.g. Chengalur *et al.* (1996), Kepner *et al.* (1996). However, the derived σ_1 estimate should be robust and is designed specifically for use in the filtered cosmic energy equation.

4. Application of the Filtered Energy Equation

Given the estimate of σ_1 , we have all the ingredients to apply the filtered cosmic energy equation (15). As discussed above, a suitably filtered cosmic potential energy can be derived by simply limiting the integration range of J_2 . Consider a sample j and suppose that its effective bias relative to the mass distribution is b_j (i.e. we define b_j by the expression $J_{2,j} = b_j^2 J_{2,\text{mass}}$). There is a slight ambiguity in determining the actual filtering scale associated with the cylinder used to determine σ_1 , and to avoid incurring bias associated with this uncertainty, since we know that $\Omega_{N\text{-body}} = 1$, $b_{N\text{-body}} = 1$, we can examine the ratio,

$$\left(\frac{\Omega_j}{\Omega_{N\text{-body}}} \right) \left(\frac{b_{N\text{-body}}}{b_j} \right)^2 = \tilde{\Omega} = \frac{\sigma_{1,j}^2}{\sigma_{1,N\text{-body}}^2} \frac{J_{2,N\text{-body}}}{J_{2,j}} \quad (23)$$

where we define an effective density parameter $\tilde{\Omega} \equiv \Omega_j/b_j^2$. The ratio (23) allows us to eliminate from our estimate of $\tilde{\Omega}$ any dependence on the relative filtering scales of σ_1 versus J_2 , as well as

the appropriate value of \tilde{g} , but is biased if the scale dependence in \tilde{g} is not the same in both the N-body and real catalogs. The other uncertain parameters are r_{max} , the upper limit, and r_{min} , the lower limit for evaluation of the J_2 integral. Although J_2 converges at $r = 0$, we choose $r_{min} = 0.1 \text{ h}^{-1} \text{ Mpc}$, roughly the separation of the closest pairs considered, so as to eliminate from analysis the velocity dispersion internal to galaxies and to consider only the dispersion of galaxies moving relative to each other. The appropriate r_{max} must be in the range $2 - 10 \text{ h}^{-1} \text{ Mpc}$ to match the velocity filtering, but fortunately the exact choice of r_{max} is not critical. In Table 5, this ratio is listed as a function of r_{max} for maximum projected pair separation of $2 \text{ h}^{-1} \text{ Mpc}$, using the values of σ_1 derived from Table 4. We find that the measured value of $\tilde{\Omega}$ is fortunately reasonably insensitive to variations in r_{max} for both the IRAS and UGC data. With an N-body simulation that better matched the $\xi(r)$ of observed catalogs, there would ideally be no sensitivity to the uncertain value of r_{max} .

The statistical precision of our estimate of $\tilde{\Omega}$ is determined by the statistical errors of J_2 and of σ_1 . Fisher et al (1994) estimate that σ_8 for the IRAS 1.2Jy catalog has a statistical error of 6%. We shall assume that J_2 has a similar error. The dominant statistical error is uncertainty in the estimate of σ_1 , which leads to a statistical precision of 34% for the measurement of $\tilde{\Omega}$ for the IRAS and UGC samples. Larger, denser samples of galaxies should enable one to greatly improve the quality of the $G(\Delta v)$ distribution and to greatly reduce the statistical uncertainty of $\tilde{\Omega}$.

Table 5 shows that both the IRAS and UGC catalogs lead to estimates $\tilde{\Omega} \approx 0.14$. Given the known $J_2(r)$ functions for the IRAS and UGC surveys, one would have naively expected to find $\tilde{\Omega}_{iras}/\tilde{\Omega}_{ugc} = (b_{ugc}/b_{iras})^2 \approx 1.7$, where the latter follows from the known $\xi(r)$ and σ_8 values for the two catalogs (Fisher *et al.* 1994). The contrary result demonstrates that both catalogs cannot be linearly biased tracers of the mass distribution. In fact, it is likely that neither sample is a linearly biased mass tracer on the small scale we are probing in this analysis.

5. Discussion and Conclusions

We have developed a single galaxy weighted statistic, σ_1 , which contains much of the same information as the traditional pair weighted statistic, $\sigma_{12}(r)$, but we believe the new statistic will prove to be much more stable than $\sigma_{12}(r)$. We have computed a galaxy weighted measure of the galaxy pair dispersion for a semi-volume limited catalogs of 2374 IRAS galaxies and 1959 UGC galaxies. For the IRAS sample, we find a value for the one-particle one-dimensional velocity dispersion of $\sigma_1 = 96 \pm 16 \text{ km/sec}$ based on analysis of galaxy pairs with projected separation, $r_p < 2 \text{ h}^{-1} \text{ Mpc}$ and line-of-sight separation less than or equal to 1000 km/sec , while our best estimate of σ_1 for the UGC sample is $130 \pm 15 \text{ km/s}$. The higher value for UGC is not unexpected, given that it better samples the hot centers of clusters of galaxies than does the IRAS survey. These velocity dispersions are appropriate for use in a filtered version of the Layzer-Irvine equation and lead to an estimate of the density parameter, $\tilde{\Omega} \equiv \Omega/b^2$. As usual there is a degeneracy between bias in the galaxy tracer and Ω . Our best estimate for both the IRAS and UGC catalog is $\tilde{\Omega} \approx 0.13 - 0.17$, consistent with some recent determinations on this scale (Fisher *et al.* 1994, Carlberg *et al.* 1996, Fisher and Nusser 1996). It is encouraging that the results for $\tilde{\Omega}$ obtained using the more densely sampled optical catalog seem to be roughly consistent with those obtained using the IRAS galaxies, in spite of the differences in their J_2 integrals, but at the same time, this consistency shows the inadequacy of the naive concept of linearly biased tracers of the mass field.

Our results clearly demonstrate that $\Omega = 1$ N-body models, normalized with mass correlation functions close to that observed in the galaxy distribution, have a one particle rms velocity that is more than twice that observed in the galaxy distribution. The particle mass of the nbody models used here is $6 \cdot 10^{12} M_{\odot}$, so that internal velocities within individual galaxies do not significantly affect our estimate of σ_1 . Note also that σ_1 for the cooled N-body catalogs, when multiplied by 2 to correct for the cooling and by 1.19 to reinsert the bias factor, is very close to the internal velocity dispersion of 450 km/s listed in Table 2 for the small scale velocity dispersion of the real space (uncooled) N-body catalog. It thus appears that our estimator of σ_1 is capable of an accurate measurement of σ_1 in the range 0–300 km/s. For optimal determination of larger values of σ_1 , a larger limit to Δv for the pair counts would be appropriate, but this is only possible for larger, deeper redshift catalogs.

This statistic has a significant advantage over $\sigma_{12}(r)$ in that it weights each galaxy equally and is not dominated by the abundant pairs in rich cluster centers, where the velocity dispersion is known to be much higher than average. The statistic should be much more robust to the inclusion of rare clusters than is $\sigma_{12}(r)$. Given that the J_2 integral on small scales is known to be very stable from one catalog to another, further estimates of σ_1 , combined with the filtered cosmic energy equation, should lead to a reliable estimate of the effective $\tilde{\Omega}$ on the scale of a few Mpc.

The method we describe for estimation of σ_1 has the disadvantage that we have deleted the majority of galaxies from consideration because they have too few neighbors. Variations on our procedure might well turn out to be more suitable for larger catalogs. However, preliminary estimates (Davis *et al.* 1997) derived from the large LCRS survey (Shectman *et al.* 1996) indicate that this problem is overcome with the dense sampling of LCRS; most galaxies have sufficient neighbors in this densely sampled survey to be included and the derived σ_1 is very stable.

The “coldness” of the typical thermal environment of galaxies has been noted for quite some time (Peebles 1992; Ostriker and Suto 1990). Most previous estimates of the small scale velocity field have been based on the observed pair dispersion σ_{12} , which is perhaps suspect. The results presented here imply that the low rms velocity of galaxies relative to their neighbors is not simply a problem of the inclusion or absence of a sufficient number of rare, rich clusters. The average galaxy in a typical group has a local velocity field that is much colder than expected in high Ω models; the mock catalogs demonstrate the problem very clearly. Further evidence for a cold velocity field comes from Tully-Fisher distance estimates using such sophisticated statistical procedures as the VELMOD algorithm described by Strauss and Willick (1995). Willick *et al.* (1996) suggest a very similar small scale random velocity, $\sigma_1 \approx 125 \pm 20$ km/s, although the weighting and filtering of their estimate are rather different from those of the measure we present here.

Another argument for cold velocity fields is the remarkably quiet Hubble flow in the vicinity of the Local Group of galaxies; the rms peculiar velocity of galaxies within $5h^{-1}$ Mpc of the Milky Way is only 60 km/s (Schlegel *et al.* 1994). This result is extremely difficult (Schlegel *et al.* 1994), if not impossible (Govertano *et al.* 1996) to reconcile with any N-body simulation for an open or closed Universe! Understanding why the observed small scale velocity field is so cold remains one of the major unsolved mysteries of large scale structure.

The quantity measured in our analysis, Ω/b_j^2 , is formally very nearly equal to the square of $\beta \equiv \Omega^{0.6}/b_j$, the quantity measured in the analyses of large scale flows; however, this analogy presumes that the bias factor b has the same meaning on these very different scales. The IRAS results quoted here are consistent with $\beta \approx 0.30 - 0.35$, assuming a scale-independent bias.

This value is somewhat lower than that derived from recent comparisons of observed peculiar velocities and the IRAS predicted gravity field (Davis, Nusser and Willick 1996; Willick *et al.* 1996). This modest difference between a measurement on scales of $1-2h^{-1}$ Mpc, and another with an effective scale in the range $10-50h^{-1}$ Mpc, is perhaps the signature of scale-dependent bias, as discussed recently by Kauffmann *et al.* (1996). A modest trend of increasing Ω estimates with measurement scale would also be expected in mixed dark matter models with $\Omega_\nu \approx 0.2-0.3$ (Primack 1994; 1996) in which there is some suppression of growth within galaxy-sized halos; on the scale of the large-scale flows, the dark matter should fully participate in the clustering and the measured β should reach its asymptotic limit.

The cold thermal environment of the local galaxy distribution implies either that the galaxies are a strongly biased tracer on small scales and that the mass normalization is $\sigma_8 < 0.4$ in an $\Omega = 1$ model, or that $\Omega \approx 0.15-0.4$ with the galaxies roughly tracing the mass distribution, perhaps with modest bias on small scale. The former conclusion is rather far from the COBE suggested normalization in many (although not all) models of large scale structure (Bunn, Scott, and White, 1995), and the latter suggestion, while consistent with many observations, is not consistent with the higher values derived from the POTENT analysis on larger scale (Dekel *et al.* 1993), nor is it consistent with the naive expectations from inflation. Neither $\Omega = 1$ and $\sigma_8 \leq 0.4$ nor $\Omega \leq 0.25$ and $\sigma_8 = 1$ appears consistent with the observed abundance of rich galaxy clusters (White *et al.* 1993). Low values of Ω have the additional problem of an overly steep mass auto-correlation function, which requires galaxies to be anti-biased ($b < 1$) on small scales (e.g. Davis *et al.* 1985; Klypin, Primack, & Holtzman 1995; Cole *et al.* 1997), a difficulty which has been known but neglected for years. Such an antibias will be difficult to reconcile with the already low values of Ω derived here.

ACKNOWLEDGEMENTS

We acknowledge helpful conversations with M. White, S. Zaroubi, and M. Craig. This work was supported in part by NSF grant AST95-28340.

Table 1 $K/|W|$ from nbody simulations

		$\Omega = 1, n=-1$	$\Omega = 0.1, n=-1$	$\Omega = 1, \text{CDM}$
σ_s/r_0	K_{small}	$(K/W)_{small/large}$	$(K/W)_{small/large}$	$(K/W)_{small/large}$
.6	7.8	0.78/0.58	0.71/0.36	0.92/0.42
1.2	8.9	0.73/0.63	0.65/0.41	0.79/0.48
2.4	10.6	0.73/0.66	0.63/0.42	0.75/0.52
4.8	12.5	0.73/0.67	0.62/0.42	

Table 2 Scale dependence of internal and external dispersion of mock catalog

Scale (Mpc) radius	$\sigma(\Delta v_p)$ internal	$\sigma(\bar{v}_p)$ external	σ_{rms}	fraction	$\frac{\sigma_{with\ neighbors}}{\sigma_{total}}$
1	458	420	667	0.29	1.23
2	451	407	640	0.43	1.18
3	436	389	604	0.56	1.11
4	425	372	577	0.69	1.06
5	418	365	562	0.80	1.04
all particles			541		

Table 3 Fractions with excess neighbors in the catalogs (redshift space)

Survey	fraction with neighbors	$\frac{\sigma_{with\ neighbors}}{\sigma_{total}}$
N-body	0.28	1.19
IRAS	0.25	
UGC	0.29	

Table 4 Dispersion Results (exponential & gaussian models)

	σ_I (exponential)	σ_I (gaussian)	σ_1
IRAS	180^{+35}_{-20}	160^{+15}_{-30}	95 ± 16
UGC	220^{+30}_{-20}	180^{+25}_{-20}	130 ± 15
N - body	1000^{+200}_{-90}	540^{+80}_{-45}	325^{+40}_{-27}
N - bodycooled	500^{+25}_{-45}	320 ± 10	190 ± 10

Table 5 $\tilde{\Omega}$ versus r_{max}

r_{max} ($h^{-1} Mpc$)	IRAS	UGC
2	0.17	0.14
4	0.14	0.13
6	0.13	0.12

References

- Bean A. J., Efstathiou G., Ellis R. S., Peterson B. A., Shanks T. 1983, MNRAS, 205, 605
- Bartlett, J.G., & Blanchard, A. 1993, in “Cosmic Velocity Fields: IAP 1993”, ed. F. Bouchet & M Lachièze-Rey, Editions Frontieres, p. 281.
- Bartlett, J.G., & Blanchard, A. 1996, A&A, 307, 1
- Brainerd, T.G., Bromley, B.C., Warren, M.S., & Zurek, W.H. 1996, Ap.J. 464, L103
- Bunn, E. F., Scott, D., & White, M. 1995, Ap.J. 441, L9
352, L29.
- Carlberg, R, Yee, H., Ellingson, E., Abraham, R., Gravel, P., Morris, S., & Pritchet, C. J. 1996, Ap.J. 462, 32
- Chengalur, J.N., Salpeter, E.E., & Terzian, Y. 1996, ApJ., 461, 546
- Cole, S., Weinberg, D.H., Frenk, C.S., & Ratra, B. 1997, astro-ph/9702082
- Davis M., Geller M., and Huchra J. P. 1978, ApJ, 221, 1
- Davis M. and Peebles P. J. E. 1977, ApJS, 34, 425
- Davis M. and Peebles P. J. E. 1983, ApJ, 267, 465. (DP83)
- Davis M., Efstathiou G., Frenk C. S. and White S. D. M. 1985, Ap J 292, 371-394.
- Davis M., Nusser A., and Willick 1996, Ap.J., 473, 22
- Davis, M., Lin, H., & Kirshner, R. 1997, in preparation
- Dekel A., Bertschinger E., Yahil A., Strauss M.A., Davis M., Huchra J. P. 1993, Ap J, 412, 1-21.
- de Lapparent V., Geller M., and Huchra J. 1988, ApJ, 332, 44
- Fall S. M. 1976, MNRAS, 172, 23p
- Fisher K. B. 1992, PhD thesis, University of California, Berkeley
- Fisher K. B., Davis M., Strauss M. A., Yahil A., Huchra J. P. 1994, MNRAS, 266, 50 (Fisher et. al. I)
- Fisher K. B., Davis M., Strauss M. A., Yahil A., and Huchra J. P. 1994, MNRAS, 267, 927 (Fisher et. al. II)
- Fisher K. B., Huchra J. P., Strauss M. A., Davis M., Yahil A., and Schlegel D. 1995, Ap J Supp., 100, 69-103.
- Fisher K., and Nusser A. 1995, preprint astro-ph/9510049
- Gelb J. M. and Bertschinger E. 1994, Ap J. 436, 467-490.
- Gelb J. M. and Bertschinger E. 1994, Ap J. 436, 491-508.
- Geller M., and Peebles P. J. E. 1973, Ap J., 184, 329
- Govertano, F., Moore, B., Cen, R., Stadel, J., Lake, G., and Quinn, T., 1996, astro-ph/9612007
- Guzzo L., Fisher K., Strauss M., Giovanelli R. Haynes M. 1996, Ap.J., 463, 395

Hale-Sutton D., Fong P., Metcalfe N., Shanks T. 1989, MNRAS, 237, 569

Juszkiewicz R, and Yahil A. 1989, Ap J. Lett., 346, L49.

Kauffmann G., Nusser A., and Steinmetz M. 1995, preprint astro-ph/9512009.

Kepner, J., Summers, F., and Strauss, M. 1996, preprint astro-ph/9607097

Klypin, A., Primack, J., & Holtzman, J. 1995, preprint astro-ph/9510024

Marzke R.O., Geller M.J., da Costa L.N., Huchra J.P. 1995, Astron. J, 110 (no.2), 447-501.

Mo H. J., Jing Y. P., and Borner G. 1993, MNRAS, 284, 703.

Mo, H. J., Jing, Y. P., and Borner, G. 1996, preprint astro-ph/9607143

Nolthenius, R, and White, S. D. M. 1987, MNRAS, 22, 505

Nolthenius, R., Klypin, A., and Primack, J. R. 1994, Ap.J. Lett., 422, L45

Ostriker J. P. and Suto Y. 1990, Ap J, 348, 378-82.

Peebles P. J. E. 1979, Astron. J, 84, 6, 730

Peebles P. J. E. 1980 "The Large-Scale Structure of the Universe". Princeton University Press, Princeton, NJ

Peebles P. J. E. 1981 Ap J, 248, 885-97.

Peebles P. J. E., 1992, in "Relativistic Astrophysics and Particle Cosmology", Texas/PASCOS 92 Symp. ed. C. W. Akerlof & M. A. Srednicki (Ann. NY Acad. Sci., vol 688), 84

Primack, J. R. 1994, in "Proceedings of the International School on Cosmological Dark Matter", ed. J. Valle, A. Perez, World Scientific, p. 81.

Primack, J.R. 1996, astro-ph/9610078

Ramella, M., Geller, M. and Huchra, J. 1989, ApJ., 344, 57

Rivolo A. R., and Yahil A. 1981, ApJ, 251, 477

Santiago B., Strauss M., Lahav O., Davis M., Dressler A., & Huchra J. 1995, Ap.J., 446, 457

Santiago B., Strauss, M. A., Lahav, O., Davis, M. Dressler, A., and Huchra, J. 1996, Ap.J., 461, 38

Schlegel, D, Davis, M., and Summers, F. 1994, Ap.J. 427, 527

Shectman, S., Landy, S.D., Oemler, A., Tucker, D.L., Lin, H., Kirshner, R.P., & Schechter, P.L. 1996, astro-ph/9604167

Somerville, R., Davis, M., & Primack, J. 1996, astro-ph/9604041

Strauss M., Yahil A., Davis M., Huchra J. 1992, ApJ 397, 395

Strauss, M., & Willick, J. 1995, Phys. Reports, 261, 271.

White, S.D.M., Efstathiou, G. and Frenk, C.S. 1993 MNRAS 262, 1023

Willick, J., Strauss, M., Dekel, A., and Kolatt, T. 1996, astro-ph/9612240

Zaritsky, D. and White, S.D.M. 1994, Ap.J. 435, 599

Zaritsky, D., Smith, R., Frenk, C., & White, S 1996, astro-ph/9611199

Zurek W. H., Quinn P. J., Salmon J. K., Warren M. S., 1994, ApJ, 431, 559

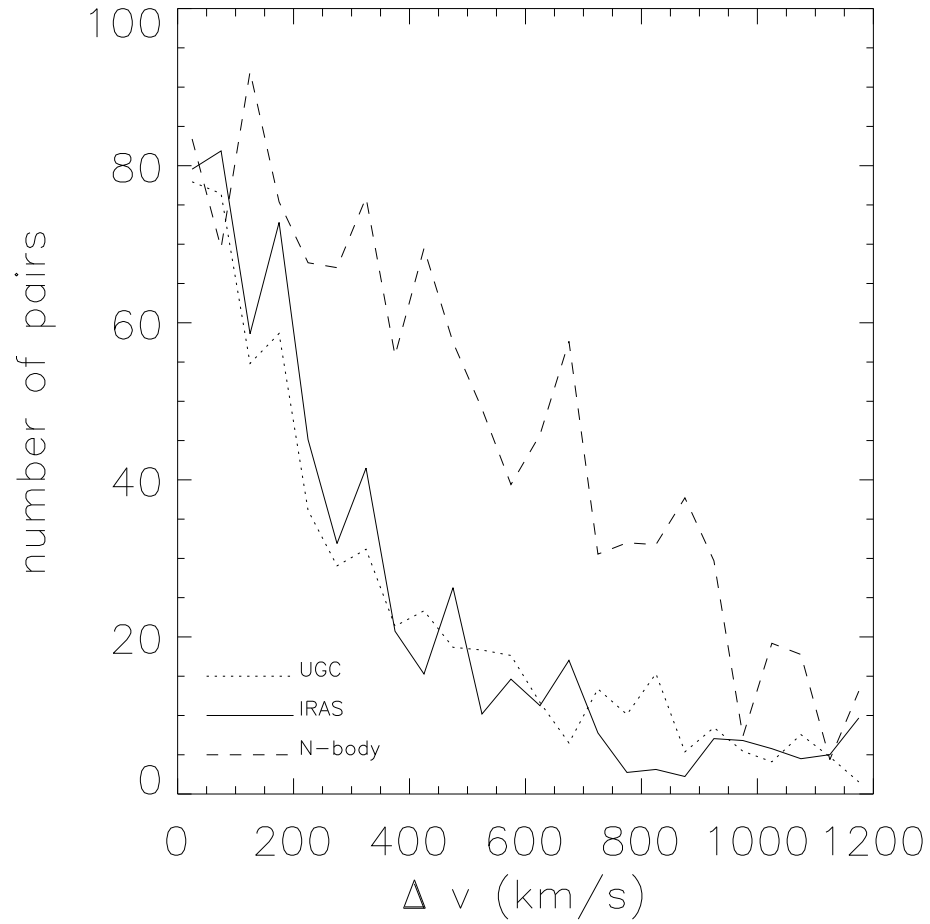


Figure 1: The distributions of the number of pairs within a cylindrical radius of $2h^{-1}$ Mpc as a function of velocity separation of the pair (galaxy-weighted).

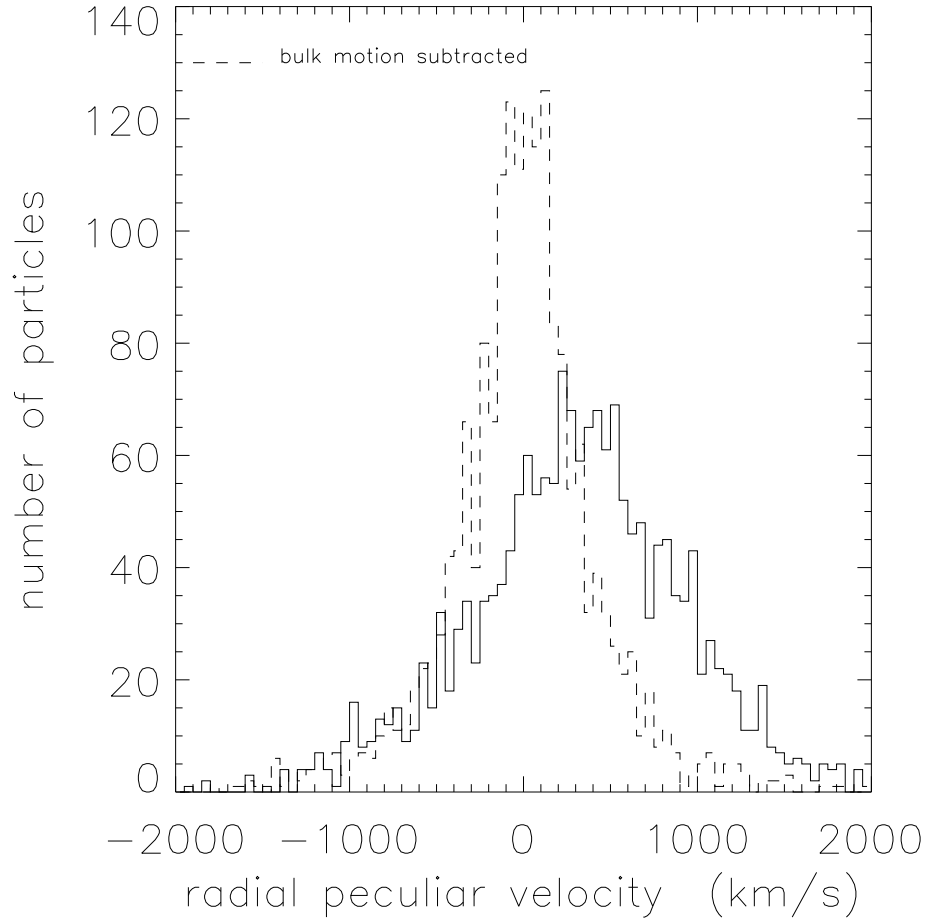


Figure 2: The radial velocity distribution function of N-body points having pairs with real space separation $r_p < 2 h^{-1}$ Mpc. The solid curve is the peculiar velocity relative to the center of the mock catalog. The dashed curve is the velocity of the point relative to the mean velocity of all points within a neighbor radius $r_p = 2h^{-1}$ Mpc.

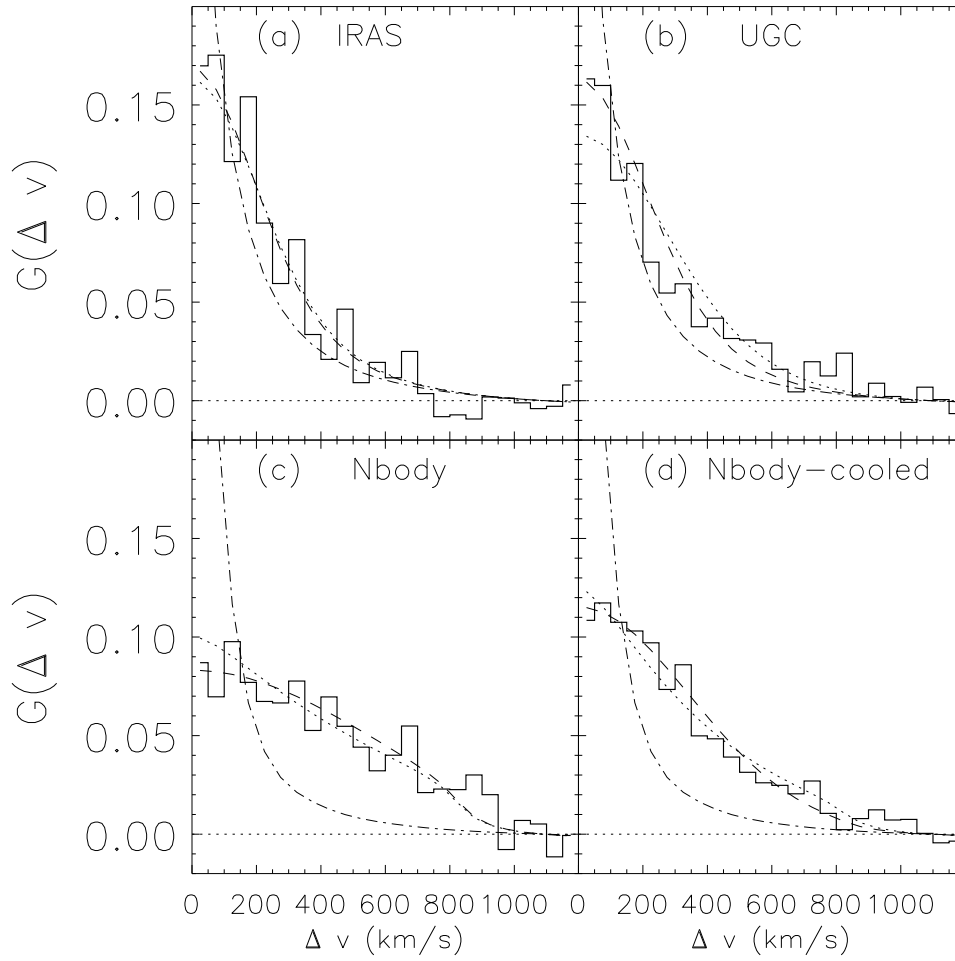


Figure 3: The observed distributions $G(\Delta v)$ plotted as solid curves along with both the best fitting Gaussian (dotted curve) and exponential models (dashed curve). The dot-dashed curve is a model with $\sigma_I = 0$. (a) IRAS (b) UGC (c) N-body (d) N-body cooled